01 Jan 2018

Efficient Inverse Design of Transonic Airfoils using Variable-Resolution Models and Manifold Mapping

Xiaosong Du
Missouri University of Science and Technology, xdnwp@mst.edu

Leifur Leifsson

Slawomir Koziel

Recommended Citation

X. Du et al., "Efficient Inverse Design of Transonic Airfoils using Variable-Resolution Models and Manifold Mapping," *AIAA Aerospace Sciences Meeting, 2018*, American Institute of Aeronautics and Astronautics, Inc., AIAA, Jan 2018.
The definitive version is available at https://doi.org/10.2514/6.2018-1051

AIAA SciTech Forum
8–12 January 2018, Kissimmee, Florida
2018 AIAA Aerospace Sciences Meeting

10.2514/6.2018-1051

Efficient Inverse Design of Transonic Airfoils Using Variable-Resolution Models and Manifold Mapping

Xiaosong Du[1], and Leifur Leifsson[2]
Computational Design Laboratory, Iowa State University, Ames, Iowa 50011

Slawomir Koziel[3]
Engineering Optimization & Modeling Center, Reykjavik University, Menntavegur 1, 101 Reykjavik, Iceland

This paper presents an efficient approach for simulation-based inverse design of airfoil shapes using variable-fidelity computational fluid dynamics models and manifold mapping (MM). Inverse design involves determining an airfoil shape fulfilling a given target performance characteristic. In particular, the pressure coefficient distribution is typically used in aerodynamic inverse design. Such a task can be challenging when using computationally expensive simulations. In the context of local optimization, the MM technique searches for a new design in the vicinity of the current design by constructing a fast multi-fidelity model, which is setup by the available evaluations of each of the high- and low-fidelity models at the current design. The MM-based multi-fidelity model predicts the high-fidelity model response at the new design by evaluating the low-fidelity model at the new design and applying the MM mapping. The MM-based multi-fidelity model is embedded within the trust-region algorithm and terminates based on the convergence of the argument, objective, and trust-region radius to yield the optimal design. The MM-based multi-fidelity algorithm only needs one high-fidelity model evaluation per design iteration. The proposed approach is illustrated on the inverse design of airfoils in transonic inviscid flow with the NACA 2412 airfoil as baseline and the pressure distribution of the RAE 2822 airfoil at Mach 0.734 and lift coefficient 0.824 as the target. Using eight B-spline design variables, the results indicate the MM technique is able to reach the target distribution at a low computational cost when compared to derivative-free local search.

Nomenclature

A	=	non-dimensional cross-section area of current design, scalar, [-]
A_{min}	=	non-dimensional minimum cross-section area, scalar, [-]
$\mathbf{c}$	=	coarse model (low-fidelity model)
C_d	=	drag coefficient, scalar, [-]
	=	$d/(1/2\rho_\infty V_\infty^2 S)$
C_l	=	lift coefficient, scalar, [-]
	=	$l/(1/2\rho_\infty V_\infty^2 S)$
C_l^t	=	target lift coefficient, scalar, [-]
$\mathbf{C_p}$	=	pressure distribution of current design, vector, [-]
	=	$(p\text{-}p_\infty)/(1/2\rho_\infty V_\infty^2)$
$\mathbf{C_p^t}$	=	vector containing target pressure distribution, units: 1
d.c	=	drag count
	=	ΔC_d = 1E-4
$\mathbf{f}$	=	fine model (high-fidelity model)
d	=	drag force, scalar, [N]
l	=	lift force, scalar, [N]

[1] Graduate Student, Department of Aerospace Engineering, Student Member AIAA.
[2] Assistant Professor, Department of Aerospace Engineering, Senior Member AIAA.
[3] Professor, School of Science and Engineering, Senior Member AIAA.

g	=	vector containing inequality constraints
h	=	vector containing equality constraints
H	=	scalar valued objective function
i	=	index of optimal design found within each optimization step
l	=	vector containing lower bounds
l.c.	=	lift count
	=	ΔC_l = 1E-2
M_∞	=	scalar valued free-stream Mach number, [-]
N_c	=	number of coarse model evaluations
N_f	=	number of fine model evaluations
p	=	static pressure at evaluated point, scalar, [Pa]
p_∞	=	free-stream static pressure, scalar, [Pa]
ρ_∞	=	free-stream fluid density, scalar, [kg/m^3]
s	=	surrogate model
S	=	reference area, scalar, [m^2]
S	=	correction matrix in manifold mapping method
u	=	vector containing upper bounds
u	=	speed relative to fluid, units: m/s
V_∞	=	free-stream velocity, units: m/s
x	=	vector of design variables
α	=	scalar valued angle of attack, scalar, [deg]
ρ	=	mass density of fluid, scalar, [kg/m^3]

Abbreviation

HPC	=	*High-Performance Computation*
MM	=	Manifold Mapping
PS	=	Pattern Search

I. Introduction

Traditional airfoil design optimization[1] can be broadly classified into direct design optimization[2] and inverse design[3]. The direct optimization aims at maximizing or minimizing one (or a set of) specific performance parameter(s), such as the lift and drag coefficient(s). The other type of design method, inverse design, combines the simulation model with the experience of the designer by design the shape to yield desired characteristics. For both types of optimizations, many advanced methods, such as gradient-based search[4] and adjoint-based search[5,6], have been developed. Many of these methods need gradient information from model solver, which may or may not be available.

Surrogate-based methods are useful for speeding up simulation-based design optimization[8,9]. Multi-fidelity modeling techniques[10] are particularly efficient for local optimization. Those types of techniques reduce the amount of high-fidelity model information required to setup a reliable model compared to approximation-based methods by encoding knowledge of the system physics within the multi-fidelity model using a hierarchy of low- and high-fidelity models. This reduces the overall optimization cost.

This work describes an efficient approach for aerodynamic inverse design optimization with variable-fidelity models and the manifold mapping technique[11]. The paper gives the technical details of the approach, and illustrates it on a design problem involving inverse design of airfoils in inviscid transonic flow.

II. Formulation of the Inverse Design Problem

This work considers nonlinear PDE-constrained optimization problems of the form[12]

$$\mathbf{x}^* = \arg\min_{\mathbf{l}\le\mathbf{x}\le\mathbf{u}} H(\mathbf{f}(\mathbf{x})) \text{ s.t. } \mathbf{g}(\mathbf{x}) \le 0, \mathbf{h}(\mathbf{x}) = 0, \tag{1}$$

where **x** is the design variable vector, $\mathbf{x}^*$ is the optimized design, H is a scalar valued objective function, **f**(**x**) is a vector with the figures of merit, **g**(**x**) is a vector with the inequality constraints, **h**(**x**) is a vector with the equality constraints, and **l** and **u** are the design variable lower and upper bounds, respectively.

In inverse airfoil design, the goal is to determine the airfoil shape $\mathbf{x}^*$ yielding a given target pressure coefficient distribution C_p^t (which describes the non-dimensional pressure acting normal to the surface of the airfoil). In this work, the objective function is written as

$$H(\mathbf{f}(\mathbf{x})) = \left\| C_p(\mathbf{x}) - C_p^t \right\|^2, \tag{2}$$

where $C_p(\mathbf{x})$ is the pressure coefficient distribution for the current design $\mathbf{x}$. The constraints of interest may include restrictions on the airfoil cross-section due to structural or volume requirements. This work considers an inequality constraint on the cross-sectional area as

$$g(\mathbf{x}) = A_{\min} - A(\mathbf{x}) \le 0, \tag{3}$$

where A_{min} is the minimum non-dimensional cross-sectional area, and $A(\mathbf{x})$ is the non-dimensional cross-sectional area of the current design $\mathbf{x}$. The lift of the airfoil depends on the angle of the attack of the flow onto the airfoil. Since the lift can be calculated directly from the target pressure coefficient distribution, an equality constraint is considered of the form

$$h(\mathbf{x}) = C_l^t - C_l(\mathbf{x}, \alpha) = 0, \tag{4}$$

where C_l^t is the target lift coefficient (based on the target pressure), $C_l(\mathbf{x},\alpha)$ is the lift coefficient of the current design $\mathbf{x}$ at the angle of attack α. This equality constraint is handled by using α as a dummy variable during the simulation process. This way the constraint (4) can be easily fulfilled for the current design $\mathbf{x}$.

The design problem (1) with the formulation (2)-(4) is challenging since computationally expensive simulations are needed, and the dimensionality of the design space can be large. Moreover, gradient information through efficient adjoint methods[5,6] may not be available. Therefore, this work utilizes efficient surrogate-based optimization with a hierarchy of multi-fidelity models.

III. Multi-Fidelity Design Optimization with Manifold Mapping

Solving (1) is accelerated using a multi-fidelity optimization algorithm of the form

$$\mathbf{x}^{(i+1)} = \arg\min_{\mathbf{l} \le \mathbf{x} \le \mathbf{u}} H(\mathbf{s}^{(i)}(\mathbf{x})), \tag{5}$$

where $\mathbf{x}^{(i)}$, $i = 0, 1, \ldots$, is a sequence of approximate solutions to (1), $\mathbf{l}$ and $\mathbf{u}$ are the lower and upper bounds on $\mathbf{x}$, respectively, and $\mathbf{s}^{(i)}(\mathbf{x})$ is the multi-fidelity model at design iteration i. The objective function H for inverse design is defined in the next section. The algorithm (5) is embedded within the trust-region framework[13-15]. The algorithm (5) is driven by the pattern search algorithm[12,16].

Manifold mapping[5,6] (MM) is used in this work to construct the multi-fidelity model $\mathbf{s}(\mathbf{x})$. The MM model is defined at each iteration i as

$$\mathbf{s}^{(i)}(\mathbf{x}) = \mathbf{f}(\mathbf{x}^{(i)}) + \mathbf{S}^{(i)}\left(\mathbf{c}(\mathbf{x}) - \mathbf{c}(\mathbf{x}^{(i)})\right), \tag{6}$$

where $\mathbf{S}^{(i)}$ is the correction matrix at each iteration, defined as

$$\mathbf{S}^{(i)} = \mathbf{\Delta F} \cdot \mathbf{\Delta C}^{\dagger}, \tag{7}$$

where

$$\mathbf{\Delta F} = [\mathbf{f}(\mathbf{x}^{(i)}) - \mathbf{f}(\mathbf{x}^{(i-1)}) \quad \ldots \quad \mathbf{f}(\mathbf{x}^{(i)}) - \mathbf{f}(\mathbf{x}^{(\max\{i-n,0\})})], \tag{8}$$

and

$$\mathbf{\Delta C} = [\mathbf{c}(\mathbf{x}^{(i)}) - \mathbf{c}(\mathbf{x}^{(i-1)}) \quad \ldots \quad \mathbf{c}(\mathbf{x}^{(i)}) - \mathbf{c}(\mathbf{x}^{(\max\{i-n,0\})})], \tag{9}$$

where n denotes dimensionality of the design space, and

$$\mathbf{\Delta C}^{\dagger} = \mathbf{V}_{\mathbf{\Delta C}} \mathbf{\Sigma}_{\mathbf{\Delta C}}^{\dagger} \mathbf{U}_{\mathbf{\Delta C}}^{T} \tag{10}$$

is the pseudoinverse of $\mathbf{\Delta C}$, and $\mathbf{U}_{\mathbf{\Delta C}}$, $\mathbf{\Sigma}_{\mathbf{\Delta C}}$, and $\mathbf{V}_{\mathbf{\Delta C}}$ are the factors in the singular value decomposition of the matrix $\mathbf{\Delta C}$. The matrix $\mathbf{\Sigma}_{\mathbf{\Delta C}}^{\dagger}$ is the result of inverting the nonzero entries in $\mathbf{\Sigma}_{\mathbf{\Delta C}}$, leaving the zeroes invariant.

IV. Numerical Example

The proposed approach is illustrated on a numerical example involving the inverse design of transonic airfoil shapes. This section gives the details of the problem statement, modeling approach, and optimization results.

A. Problem Statement

Inverse design of airfoils in transonic inviscid flow is considered using the NACA 2412 airfoil as a baseline and the pressure distribution of the RAE 2822 airfoil as the target. The Mach number is $M_\infty = 0.734$, and the lift coefficient is $C_l = 82.4$ l.c. (where 1 l.c. = 1 lift count = 1.0E−2). The objective is to minimize the norm of the difference between the target distribution and the pressure distribution of the given airfoil shape (cf. (2)). The design variables are the vertical coordinates of eight control points in a B-spline airfoil shape parameterization constrained to be within upper and lower bounds of 0.1 and −0.1, respectively (Fig. 1a).

B. Computational Modeling

The compressible Euler equations are solved on an O-type mesh (Fig. 1b) using the Stanford University Unstructured code[17]. This O-type method, generated from Pointwise, has the far-field boundary as 55 chord lengths away from the airfoil surface, and the first-layer mesh thickness as 0.0004 chord length. The high-fidelity model ($\mathbf{f}(\mathbf{x})$) uses a 512 × 512 mesh, due to fixed-C_l grid convergence study on RAE2822, where difference of drag coefficient between 512 × 512 mesh and 1024 × 1024 mesh is within 0.1 drag counts. In contrast, the low-fidelity model ($\mathbf{c}(\mathbf{x})$) uses a 64 × 64 mesh, due to its efficiency, taking only 1.1 minutes in grid convergence study case, and better accuracy than 32 × 32 mesh.

C. Optimization Results

The optimization problem is solved using the MM technique, taking 512 × 512 mesh as high-fidelity model and 64 × 64 mesh as low-fidelity model, as well as directly applying the pattern search (PS)[12,16] algorithm, using 512 × 512 mesh only. Both approaches do not use gradients. Figure 2 gives the evolution of the optimization run, as well as the initial and optimized shapes and responses. Figure 3 gives contour plots of the Mach number in the vicinity of the airfoil shapes. Table 1 summarizes the computational cost.

It can be observed that the MM algorithm converges relatively smoothly, but the PS algorithm does not converge fully (Fig. 2). The MM optimum matches closely to the target distribution, whereas the PS optimum is far away from the target (Fig. 3). The MM needed 8 high-fidelity simulations and 1,635 low-fidelity model evaluations, taking around 47 hours on a 32-processor high-performance computation (HPC) cluster (Table 1). PS was terminated after 15 design iterations using 781 high-fidelity simulations, taking around 482 hours. In this case, the physics-based search is more than an order of magnitude faster than the direct one.

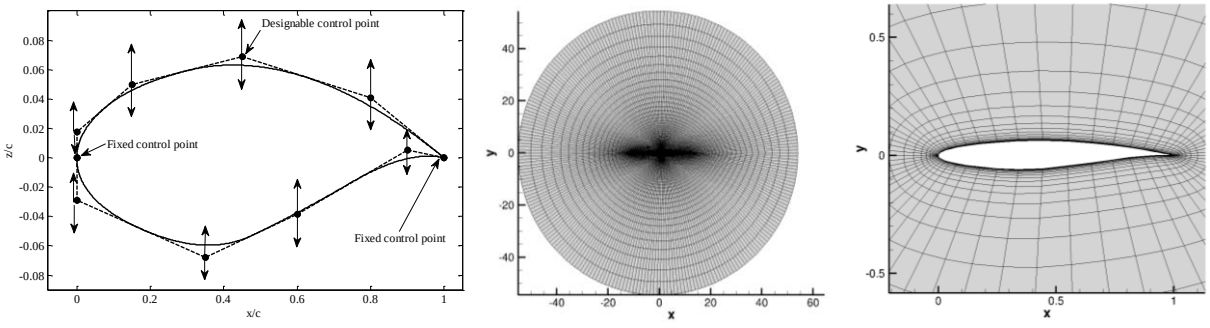

(a) (b)

Figure 1. Airfoil problem setup: (a) airfoil shape parameterization, (b) O-type computational mesh.

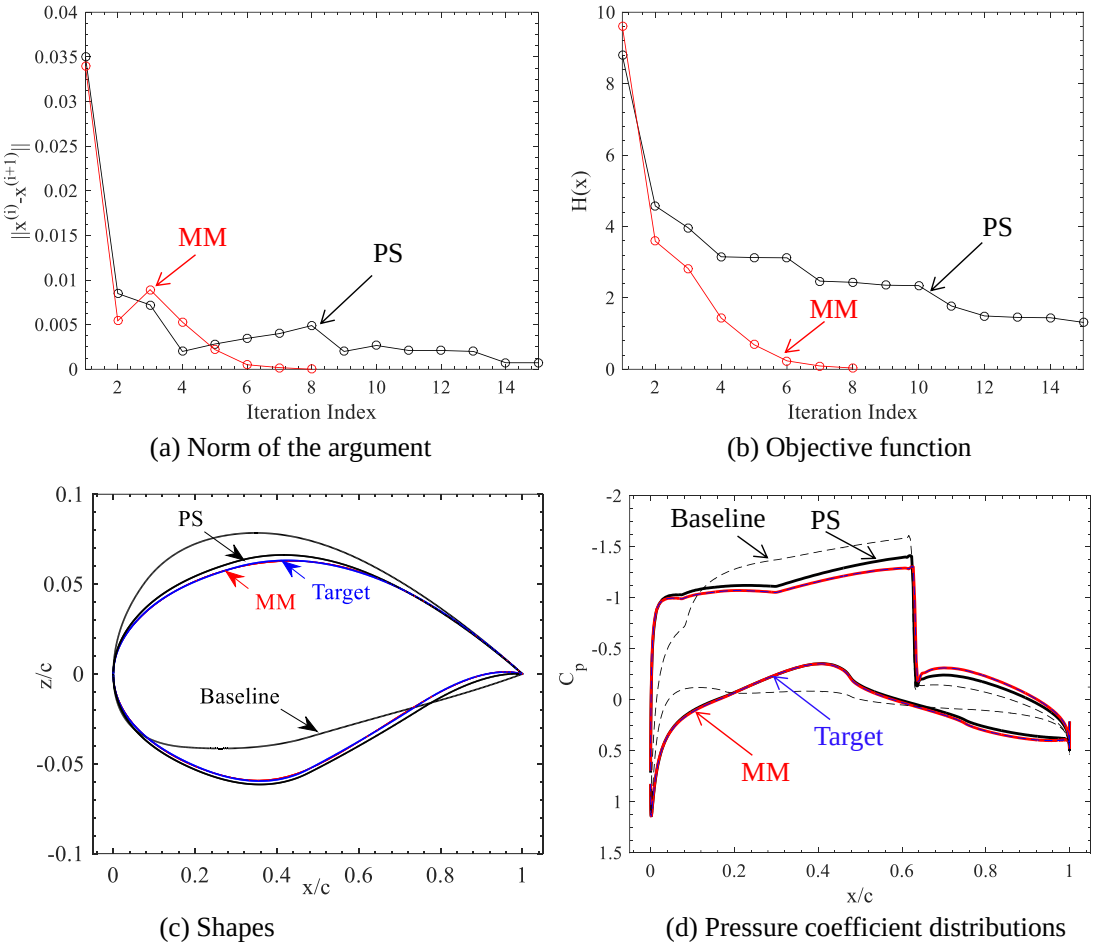

Figure 2. Optimization histories and characteristics of the designs.

Table 1: Optimization results.

Parameter/Method	Baseline (NACA 2412)	Target (RAE 2822)	Pattern Search (PS)	Manifold Mapping (MM)
C_d (d.c.)	331.8	76.3	120.7	76.3
A	0.0817	0.0779	0.0812	0.0780
N_c	–		–	1,635
N_f	–		781	8
CPU Time (hours)	–		481.7	47.0

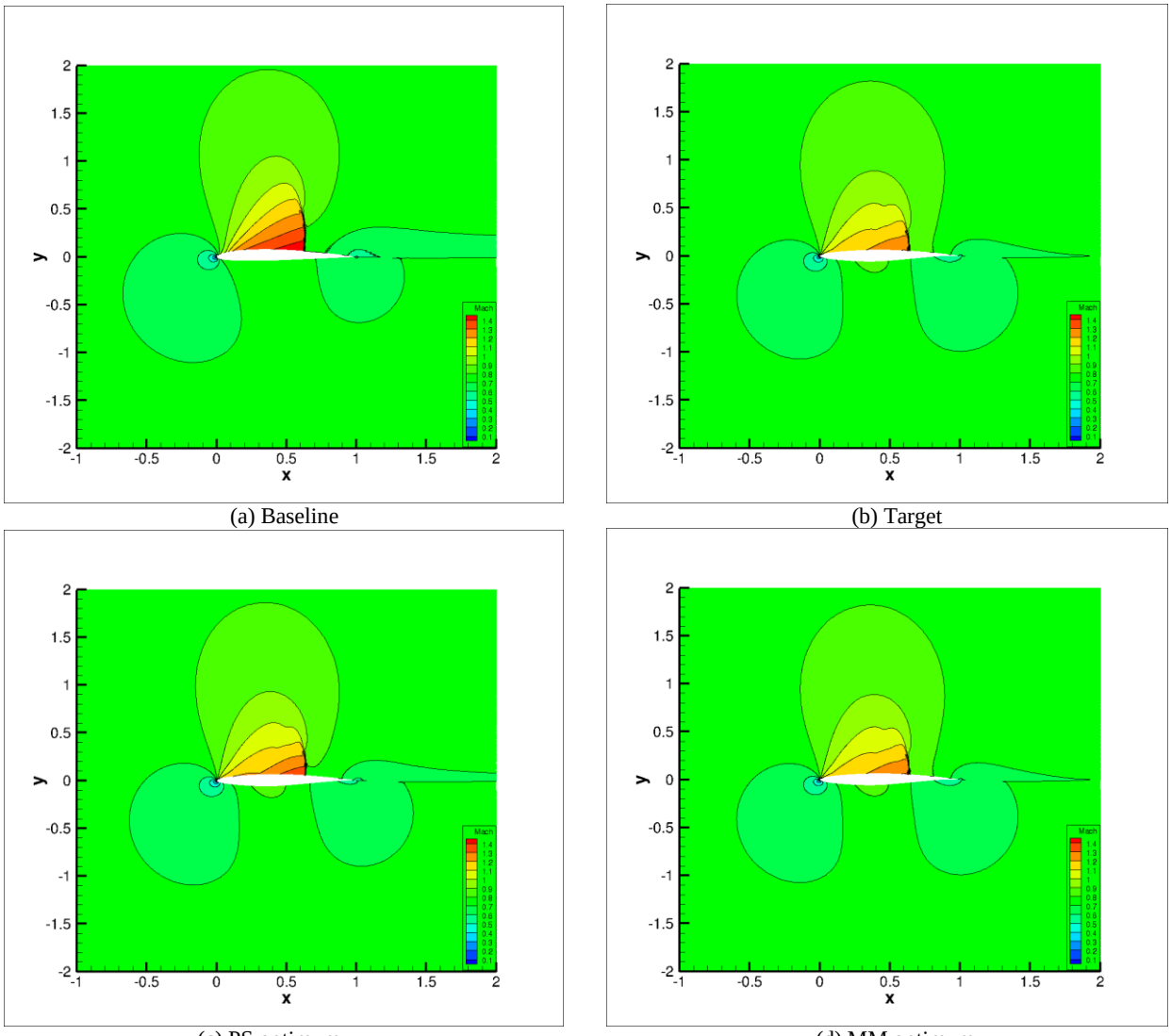

(a) Baseline (b) Target

(c) PS optimum (d) MM optimum

Figure 3. Mach number contour plots in the vicinity of the baseline, target, and optimized airfoils.

V. Conclusion

The manifold mapping technique is used for aerodynamic inverse design optimization with variable-resolution computational fluid dynamics models, multi-fidelity trust-region algorithm, and a local search technique. The results of the numerical example show that the approach yields satisfactory designs at low cost. Sensitivity information is not required in the optimization process. Future work will investigate the scalability of the approach to large-scale simulation problems.

References

[1]Jameson, A., "Aerodynamic Design via Control Theory," *Journal of Scientific Computing*, Vol. 3, 1988, pp. 233-260.

[2]Jameson, A., "Advances in Aerodynamic Shape Optimization," In: Groth C., Zingg D.W.(eds) Computational Fluids Dynamics, 2004, Springer, Berlin, Heidleberg.

[3]Zhang, M., Rizzi, A. and Nangia, R., "Transonic Airfoil and Wing Design Using Inverse and Direct Methods," AIAA 2015-1943, *SciTech, 53rd AIAA Aerospace Sciences Meeting*, Kissimmee, Florida, Jan., 2015.

[4]Hicks, R.M., and Henne, P.A, "Wing Design by Numerical Optimization," Journal of Aircraft, Vol. 15, No. 7, 1978, pp. 407-412.

[5]Kim, S., Alonso, J.J., and Jameson, A., "Design Optimization of High-Lift Configurations Using a Viscous Continuous Adjoint Method," AIAA 2002-0844, *AIAA 40th Aerospace Sciences Meeting & Exhibit*, Reno, NV, Jan. 2000.

[6]Nemec, M., and Zingg,. D.W., "Optimization of high-lift configurations using a Newton-Krylov algorithm," *16th AIAA Computational Fluid Dynamics Conference*, Orlando, FL, Jun. 23-26, 2003

[7]Ren, J., Thelen, A., Amrit, A., Du, X., and Leifson, L., "Application of Multifidelity Optimization Techniques to Benchmark Aerodynamic Design Problems," AIAA-2016-1542, *AIAA Aerospace Sciences Meeting*, San Diego, CA, Jan. 4-8, 2016.

[8]Queipo, N.V., Haftka, R.T., Shyy, W., Goel, T., Vaidyanathan, R., and Tucker, P.K., "Surrogate-Based Analysis and Optimization," Progress in Aerospace Sciences, Vol. 41, No. 1, pp. 1-28, 2005.

[9]Forrester, A.I.J., and Keane, A.J., "Recent advances in surrogate-based optimization," *Progress in Aerospace Sciences*, Vol. 45, No. 1-3, pp. 50-79, 2009.

[10]Koziel, S., Echeverría-Ciaurri, D., and Leifsson, L. "Surrogate-based methods," in S. Koziel and X.S. Yang (Eds.) *Computational Optimization, Methods and Algorithms, Series: Studies in Computational Intelligence*, Springer-Verlag, pp. 33-60, 2011.

[11]Echeverría-Ciaurri, D., and Hemker, P.W., "Manifold Mapping: a Two-Level Optimization Technique," *Computing and Visualization in Science*, 11, pp. 193-206, 2008.

[12]Koziel, S., "Multi-fidelity multi-grid design optimization of planar microwave structures with Sonnet," *International Review of Progress in Applied Computational Electromagnetics*, Tampere, Finland, 719-724, 2010.

[13]Conn, A.R., Gould, N.I.M., and Toint, P.L., *Trust Region Methods*, MPS-SIAM Series on Optimization, 2000.

[14]Yuan, Y., "Recent advances in trust region algorithms," Mathematical Programming: Series A and B, Vol. 151, Issue 1, pp 249-281, June 2015.

[15]Schulman, J., Levine S., Moritz, P., Jordan, M., Abbeel, P., "Trust Region Policy Optimization," *Proceedings of the 31th international Conference on Machine Learning*, Vol. 37, Lille, France, 2015.

[16]Torczon, V., "On the Convergence of Pattern Search Algorithms," Society for Industrial and Applied Mathematics Journal on Optimization, Vol. 7, No. 1, pp 1-25, February, 1997.

[17]Palacios, F., Colonno, M. R., Aranake, A. C., Campos, A., Copeland, S. R., Economon, T. D., Lonkar, A. K., Lukaczyk, T. W., Taylor, T. W. R., and Alonso, J. J., "Stanford University Unstructured (SU2): An open-source integrated computational environment for multi-physics simulation and design," AIAA Paper 2013-0287, *51st AIAA Aerospace Sciences Meeting and Exhibit*, Grapevine, Texas, USA, 2013.